

A genome-wide association study in autoimmune neurological syndromes with anti-GAD65 autoantibodies

Christine Strippel,^{1,†} Marisol Herrera-Rivero,^{2,†} Mareike Wendorff,³ Anja K. Tietz,⁴ Frauke Degenhardt,³ Anika Witten,² Christina Schroeter,^{1,5} Christopher Nelke,^{1,5} Kristin S. Golombeck,^{1,5} Marie Madlener,⁶ Theodor Rüber,^{7,8} Leon Ernst,⁷ Attila Racz,⁷ Tobias Baumgartner,⁷ Guido Widman,⁷ Kathrin Doppler,⁹ Franziska Thaler,^{10,11} Kai Siebenbrodt,⁸ Andre Dik,^{1,5} Constanze Kerin,¹ Saskia Räuber,^{1,5} Marco Gallus,¹ Stjepana Kovac,¹ Oliver M. Grauer,¹ Alexander Grimm,¹² Harald Prüss,¹³ Jonathan Wickel,¹⁴ Christian Geis,¹⁴ Jan Lewerenz,¹⁵ Norbert Goebels,⁵ Marius Ringelstein,^{5,16} Til Menge,^{5,16} Björn Tackenberg,¹⁷ Christoph Kellinghaus,¹⁸ Christian G. Bien,¹⁹ Andrea Kraft,²⁰ Uwe Zettl,²¹ Fatme Seval Ismail,²² Ilya Ayzenberg,^{23,24} Christian Urbanek,²⁵ Kurt-Wolfram Sühs,²⁶ Simone C. Tauber,²⁷ Sigrid Mues,^{22,28} Peter Körtvélyessy,^{13,29} Robert Markewitz,³⁰ Asterios Paliantonis,³¹ Christian E. Elger,⁷ Rainer Surges,⁷ Claudia Sommer,⁹ Tania Kümpfel,^{10,11} Catharina C. Gross,¹ Holger Lerche,¹² Jörg Wellmer,²² Carlos M. Quesada,³² Florian Then Bergh,³³ Klaus-Peter Wandinger,³⁰ Albert J. Becker,³⁴ Wolfram S. Kunz,⁷ Gerd Meyer zu Hörste,¹ Michael P. Malter,⁶ Felix Rosenow,⁸ Heinz Wiendl,¹ Gregor Kuhlenbäumer,⁴ Frank Leypoldt,^{4,30} Wolfgang Lieb,³⁵ Andre Franke,³ Sven G. Meuth,^{1,5,†} Monika Stoll,^{2,†} and Nico Melzer^{1,5,†} on behalf of the German Network for Research on Autoimmune Encephalitis (GENERATE)

[†]These authors contributed equally to this work.

Autoimmune neurological syndromes (AINS) with autoantibodies against the 65 kDa isoform of the glutamic acid decarboxylase (GAD65) present with limbic encephalitis, including temporal lobe seizures or epilepsy, cerebellitis with ataxia, and stiff-person-syndrome or overlap forms. Anti-GAD65 autoantibodies are also detected in autoimmune diabetes mellitus, which has a strong genetic susceptibility conferred by human leukocyte antigen (HLA) and non-HLA genomic regions. We investigated the genetic predisposition in patients with anti-GAD65 AINS.

We performed a genome-wide association study (GWAS) and an association analysis of the HLA region in a large German cohort of 1214 individuals. These included 167 patients with anti-GAD65 AINS, recruited by the German Network for Research on Autoimmune Encephalitis (GENERATE), and 1047 individuals without neurological or endocrine disease as population-based controls. Predictions of protein expression changes based on GWAS findings were further explored and validated in the CSF proteome of a virtually independent cohort of 10 patients with GAD65-AINS and 10 controls. Our GWAS identified 16 genome-wide significant ($P < 5 \times 10^{-8}$) loci for the susceptibility to anti-GAD65 AINS. The top variant, rs2535288 [$P = 4.42 \times 10^{-16}$, odds ratio (OR) = 0.26, 95% confidence interval (CI) = 0.187–0.358], localized to an intergenic segment in the middle of the HLA class I region. The great majority of variants in these loci (>90%) mapped to non-coding

Received October 17, 2021. Revised February 11, 2022. Accepted March 13, 2022. Advance access publication March 28, 2022

© The Author(s) 2022. Published by Oxford University Press on behalf of the Guarantors of Brain.

This is an Open Access article distributed under the terms of the Creative Commons Attribution-NonCommercial License (<https://creativecommons.org/licenses/by-nc/4.0/>), which permits non-commercial re-use, distribution, and reproduction in any medium, provided the original work is properly cited. For commercial re-use, please contact journals.permissions@oup.com

regions of the genome. Over 40% of the variants have known regulatory functions on the expression of 48 genes in disease relevant cells and tissues, mainly CD4⁺ T cells and the cerebral cortex. The annotation of epigenomic marks suggested specificity for neural and immune cells. A network analysis of the implicated protein-coding genes highlighted the role of protein kinase C beta (PRKCB) and identified an enrichment of numerous biological pathways participating in immunity and neural function. Analysis of the classical HLA alleles and haplotypes showed no genome-wide significant associations. The strongest associations were found for the DQA1*03:01-DQB1*03:02-DRB1*04:01HLA haplotype ($P = 4.39 \times 10^{-4}$, OR = 2.5, 95%CI = 1.499–4.157) and DRB1*04:01 allele ($P = 8.3 \times 10^{-5}$, OR = 2.4, 95%CI = 1.548–3.682) identified in our cohort. As predicted, the CSF proteome showed differential levels of five proteins (HLA-A/B, C4A, ATG4D and NEO1) of expression quantitative trait loci genes from our GWAS in the CSF proteome of anti-GAD65 AINS. These findings suggest a strong genetic predisposition with direct functional implications for immunity and neural function in anti-GAD65 AINS, mainly conferred by genomic regions outside the classical HLA alleles.

- 1 Department of Neurology with Institute of Translational Neurology, University of Münster, Münster, Germany
- 2 Department of Genetic Epidemiology, Institute of Human Genetics, University of Münster, Münster, Germany
- 3 Institute of Clinical Molecular Biology, Christian-Albrechts-University of Kiel, Kiel, Germany
- 4 Department of Neurology, University of Kiel, Kiel, Germany
- 5 Department of Neurology, Medical Faculty, Heinrich-Heine University Düsseldorf, Düsseldorf, Germany
- 6 Department of Neurology, University of Cologne, Cologne, Germany
- 7 Department of Epileptology, University of Bonn, Bonn, Germany
- 8 Epilepsy Center Frankfurt Rhine-Main, Department of Neurology, University Hospital Frankfurt, and LOEWE Center for Personalized Translational Epilepsy Research (CePTER), Goethe-University Frankfurt, Frankfurt am Main, Germany
- 9 Department of Neurology, University of Würzburg, Würzburg, Germany
- 10 Institute of Clinical Neuroimmunology, University Hospital, Ludwig-Maximilians-Universität Munich, Munich, Germany
- 11 Biomedical Center (BMC), Medical Faculty, Ludwig-Maximilians-Universität Munich, Martinsried, Germany
- 12 Department of Neurology and Epileptology, Hertie Institute for Clinical Brain Research, University of Tübingen, Tübingen, Germany
- 13 Department of Neurology, Charité Universitätsmedizin Berlin, Berlin, Germany
- 14 Section of Translational Neuroimmunology, Department of Neurology, Jena University Hospital, Jena, Germany
- 15 Department of Neurology, Ulm University, Ulm, Germany
- 16 Center for Neurology and Neuropsychiatry, LVR Klinikum, Heinrich-Heine University Düsseldorf, Düsseldorf, Germany
- 17 Department of Neurology, University of Marburg/Gießen, Marburg, Germany
- 18 Department of Neurology, Klinikum Osnabrück, Osnabrück, Germany
- 19 Department of Epileptology (Krankenhaus Mara), Bielefeld University, Medical School, Campus Bielefeld-Bethel, Bielefeld, Germany
- 20 Martha Maria Hospital Halle, Halle, Germany
- 21 Department of Neurology, University of Rostock, Rostock, Germany
- 22 Department of Neurology, University Hospital Knappschaftskrankenhaus Bochum, Ruhr University Bochum, Bochum, Germany
- 23 Department of Neurology, I.M. Sechenov First Moscow State Medical University, Moscow, Russia
- 24 Department of Neurology, St Josefs Krankenhaus Bochum, Ruhr University Bochum, Bochum, Germany
- 25 Department of Neurology, Ludwigshafen Hospital, Ludwigshafen, Germany
- 26 Department of Neurology, University Hospital, MHH, Hannover, Germany
- 27 Department of Neurology, University Hospital RWTH Aachen, Aachen, Germany
- 28 Department of Neurology, University Hospital Dresden, Dresden, Germany
- 29 Department of Neurology, University Hospital Magdeburg, Magdeburg, Germany
- 30 Neuroimmunology, Institute of Clinical Chemistry, University Hospital Schleswig-Holstein, Kiel/Lübeck, Germany
- 31 Department of Neurology, Alfred-Krupp Hospital, Essen, Germany
- 32 Department of Neurology, University Hospital Essen, University of Duisburg-Essen, Essen, Germany
- 33 Department of Neurology, University of Leipzig, Leipzig, Germany
- 34 Section of Translational Epileptology, Institute of Neuropathology, University of Bonn, Bonn, Germany
- 35 Institute of Epidemiology, Christian-Albrechts-University of Kiel, Kiel, Germany

Correspondence to: Nico Melzer

Department of Neurology, Medical Faculty, Heinrich-Heine University of Düsseldorf
 Moorenstraße 5, 40225 Düsseldorf, Germany
 E-mail: nico.melzer@med.uni-duesseldorf.de

Correspondence may also be addressed to: Monika Stoll
E-mail: mstoll@uni-muenster.de

Keywords: autoimmune encephalitis; glutamic acid decarboxylase; limbic encephalitis; stiff-person syndrome; genome-wide association study

Introduction

Autoimmune neurological syndromes (AINS) are immune-mediated disorders affecting the peripheral or central nervous system or both. In the peripheral blood (PB), CSF and brain parenchyma of these patients, B cell-derived autoantibodies but also T cells recognizing a variety of neural auto-antigens can be detected, illustrating the presence of specific, humoral and cellular, adaptive immune responses.¹ AINS with autoantibodies against the 65 kDa isoform of the glutamic acid decarboxylase (GAD65) present with three clinical syndromes that can partially overlap: limbic encephalitis (LE) with temporal lobe seizures (TLS) or epilepsy (TLE), cerebellitis (CB) with cerebellar ataxia (CA), and stiff-person-syndrome (SPS).² All forms of anti-GAD65 AINS exhibit a chronic, slowly progressive disease course with limited response to immunological and symptomatic treatments, leading to severe and life-long neurologic disability. Whilst the vast majority of anti-GAD65 AINS occur in a non-paraneoplastic context, some cases may be driven by a peripheral tumour.^{2,3}

Anti-GAD65 autoantibodies also characterize autoimmune diabetes mellitus (type 1A according to the American Diabetes Association classification, T1DM). Consistently, many patients with anti-GAD65 AINS suffer from T1DM and other autoimmune endocrine disorders.⁴ Patients with anti-GAD65 AINS typically exhibit more than 100-fold higher autoantibody serum titres when compared to T1DM patients. Moreover, intrathecal autoantibody synthesis is detected in 85–100% of anti-GAD65 AINS but not in patients with T1DM only.^{2,3}

Familial cases of anti-GAD65 AINS have been associated with a rare human leukocyte antigen (HLA class II) haplotype (DRB1*15:01:01~DQA1*01:02:01~DQB1*05:02:01).⁵ In sporadic cases, both an association with HLA class II haplotypes (HLA DQA1*05:01~DQB1*02:01~DRB1*03:01)⁴ and non-HLA genes (i.e. cytotoxic T-lymphocyte-associated protein 4, CTLA4)⁶ has been found.

Here, we performed a genome-wide association study (GWAS) and analysis of the HLA region in a large German cohort of 1214 individuals, including 167 patients with sporadic anti-GAD65 AINS, to investigate the genetic basis of these disorders.

Materials and methods

Ethics, consent and permissions

Initial ethics approval was given by the ethics committee of the University of Lübeck, Germany (reference number: 13–162) and consecutively by the ethics committees of all participating centers of the German Network for Research on Autoimmune Encephalitis (GENERATE; www.generate-net.de). All participants gave written informed consent to the study.

Study population

Clinical and paraclinical data, together with DNA samples of 205 German patients of Caucasian ethnicity with anti-GAD65 AINS, were collected by the German Network for Research on Autoimmune Encephalitis (for contributing scientists see [Supplementary Table 1](#)).

We prioritized a typical clinical phenotype as primary inclusion criterion. Patients were assessed by experienced neurologists in the referring centers and classified to a phenotype, based on the involvement of either the temporal lobe (including both LE and TLE), cerebellum (CB) and spinal cord (SPS), or overlap, if more than one localization was involved.^{1–3} Clinical diagnosis was confirmed by detection of anti-GAD65 IgG autoantibodies in serum and/or CSF at least once during the disease course through a qualitative detection in a tissue-based assay (TBA) with typical staining pattern on rodent or non-human primate brain (and pancreas). To quantify antibody titres and to allow for assessment of intrathecal synthesis, a second method either a cell-based assay (CBA), enzyme-linked immunosorbent assay (ELISA) or radioimmunoassay (RIA) was added. Intrathecal synthesis of GAD65-specific IgG antibodies was assessed using the antibody-specificity index (ASI), according to Reiber with a method-specific cut-off of 4.0 (CBA) or 1.5 (ELISA, RIA).⁷

Whole blood or peripheral blood mononuclear cells from included patients were collected individually at all participating centers in EDTA tubes. DNA isolation from all patient samples was carried out using standard protocols in the Core Facility Genomics at the Medical Faculty of the University of Münster, Germany.

The control population used in this study consisted of a cohort of 1081 individuals, part of the PopGen cohort, a population-based biobank in Germany.⁸ This subset of individuals corresponded to healthy subjects without neurological or endocrine disease, age-matched to our anti-GAD65 AINS patients, with available genotype data generated on the Infinium Global Screening Array (Illumina).

Genome-wide association analysis

All patient samples were genotyped using the Infinium Global Screening Array-24 v3.0 (Illumina). Variant calling was performed with Illumina's GenomeStudio 2.0. Quality control (QC) criteria were applied separately to both patient and control cohorts and consisted of the exclusion of extra-chromosomes, of individuals with more than 1% missing genotypes, and of variants with more than 10% missingness, minor allele frequency (MAF) less than 1% and a Hardy–Weinberg equilibrium (HWE) *P*-value below 1×10^{-5} . Short insertion/deletion (indel) and multi-allelic markers were allowed. After individual QC, case and control datasets were merged, keeping only overlapping variants. The merged dataset consisted of 406 448 variants, and 1271 individuals (199 cases and 1072 controls), with a genotyping rate of 0.99899. This dataset was imputed using the Michigan Imputation Server⁹ (MIF), with the 1000 Genomes Project phase 3 v5 as reference panel, and the Minimac4 pipeline. Strand and allele flips were managed as appropriate upon QC in the MIF. Additionally, the Genotype Imputation HLA Playground (1000G deep) tool of the MIF was used to impute the HLA region.⁹ QC criteria were applied to the imputed dataset as before, with the addition of an Rsq filter to exclude variants of lesser quality (Rsq < 0.8). Outlier individuals were detected based on |Z| values

obtained for neighbour distances. Relatedness among individuals was assessed according to identity-by-descent, where a proportion threshold of 0.05 was used. For individuals showing relatedness, one individual from each pair was selected for removal according to their outlier status ($|Z|$ threshold: 6).

The final GWAS dataset consisted of 7 012 247 variants [including single nucleotide polymorphisms (SNPs) and indels] and 1214 individuals, from which 167 were cases and 1047 were controls (see Table 1 for a description of effective study population). We tested for genetic associations with anti-GAD65 AINS using an additive logistic regression model, adjusting for age, sex and the first seven dimensions coming from a principal component analysis. All QC procedures of the genotypes datasets and association analyses were performed with Plink 1.9.¹⁰ Genomic coordinates are given in the genome build GRCh37/hg19.

GWAS downstream analyses

Downstream processing of the GWAS summary statistics consisted in the definition of genomic loci that consider linkage disequilibrium (LD) information, and in performing variant annotation. Genomic loci were delineated using the SNP2GENE function of the Functional Mapping and Annotation of Genome-Wide Association Studies (FUMA GWAS) platform.¹¹ LD was defined by $r^2 \geq 0.6$ and a

window of 500 kb. LD blocks were formed with variants under the genome-wide threshold of significance ($P < 5 \times 10^{-8}$) as lead variants, and all nominally significant ($P < 0.05$) variants in the dataset that were in LD with the lead variants. As genomic loci that are constituted by a single variant, showing no support of other variants in LD with at least nominal significance, might represent false positives, unsupported loci have been omitted from this report.

Variant annotations for all variants in genomic loci were obtained with FUMA GWAS and SNPnexus.¹² These included: (i) the mapped gene up to 1 kb from gene boundaries; (ii) the localization of the variant with respect to genes (functional consequence); (iii) expression quantitative trait loci [eQTLs; false discovery rate (FDR) < 0.05] effects from the BRAINEAC (Brain eQTL Almanac) and DICE (Database of Immune Cell Expression, eQTLs and Epigenomics) databases; as well as (iv) regulatory feature reports from the ENCODE (Encyclopedia of DNA Elements) database and the Roadmap Epigenomics Project.

To shed light onto the biological context of the identified loci, a protein-protein interaction (PPI) network was created with the ReactomeFIViz app for Cytoscape v.3.7.1^{13,14} using the mapped and eQTL genes (excluding unsupported loci) as the input and adding linker genes. Clumping and module functions from this app were used to perform pathway enrichment analysis of network modules. Enriched terms were considered those with $P < 0.01$, as well as

Table 1 Basic description of the effective GWAS sample

| | GWAS sample | | | Proteomics samples | | |
|---------------------------------------|--------------------|--------------------|--------------------|--------------------|--------------------|--------------------|
| | Total | Males | Females | Total | Males | Females |
| Total | 1214 | 653 | 561 | 20 | 5 | 15 |
| Age (\pm SD) | 53.1 (\pm 14.4) | 53.8 (\pm 13.4) | 52.3 (\pm 15.4) | 44.3 (\pm 16.3) | 46.2 (\pm 20.4) | 43.6 (\pm 15.5) |
| Controls | 1047 | 602 | 445 | 10 | 3 | 7 |
| Age (\pm SD) | 53.5 (\pm 14.3) | 54.2 (\pm 13.3) | 52.6 (\pm 15.4) | 49.9 (\pm 18.2) | 56.3 (\pm 19.9) | 47.1 (\pm 18.1) |
| Cases | 167 | 51 | 116 | 10 | 2 | 8 |
| Age (\pm SD) | 50.5 (\pm 14.9) | 49.1 (\pm 13.7) | 51.1 (\pm 15.4) | 38.6 (\pm 12.8) | 31 (\pm 9.9) | 40.5 (\pm 13.3) |
| Limbic encephalitis | 101 | 35 | 66 | 10 | 2 | 8 |
| Stiff-person syndrome | 48 | 9 | 39 | 1 | 0 | 1 |
| Cerebellitis | 33 | 10 | 23 | 0 | 0 | 0 |
| Overlap | 17 | 3 | 14 | 1 | 0 | 1 |
| Type 1 diabetes mellitus | 39 | 9 | 30 | 1 | 1 | 0 |
| AID | 46 | 13 | 33 | 0 | 0 | 0 |
| Neoplasm | 15 | 6 | 9 | 0 | 0 | 0 |
| Anti-GAD65 IgG high | 120 | 33 | 87 | 5 | 1 | 4 |
| Anti-GAD65 IgG low | 47 | 18 | 29 | 5 | 1 | 4 |
| Intrathecal synthesis | 123 | 33 | 90 | 3 | 1 | 2 |
| Associated autoimmune diseases | | | | | | |
| Autoimmune thyroid disease | 34 | – | – | – | – | – |
| Hashimoto's disease | 31 | – | – | – | – | – |
| Graves' disease | 3 | – | – | – | – | – |
| Vitiligo | 8 | – | – | – | – | – |
| Inflammatory bowel disease | 4 | – | – | – | – | – |
| Ulcerative colitis | 3 | – | – | – | – | – |
| Crohn's disease | 1 | – | – | – | – | – |
| Autoimmune gastritis | 6 | – | – | – | – | – |
| Sjögren syndrome | 3 | – | – | – | – | – |
| Addison's disease | 2 | – | – | – | – | – |
| Ankylosing spondylitis | 1 | – | – | – | – | – |
| Primary biliary cholangitis | 1 | – | – | – | – | – |
| Polymyalgia rheumatica | 1 | – | – | – | – | – |
| Primary sclerosing cholangitis | 1 | – | – | – | – | – |
| Psoriasis | 1 | – | – | – | – | – |
| Rheumatoid arthritis | 1 | – | – | – | – | – |

AID = autoimmune disorders other than type 1 diabetes mellitus; Overlap = any combination of LE, SPS and CB; SD = standard deviation.

number of overlapping genes (n) > 2 in modules 0–3 and $n=2$ in modules 4–5. Moreover, pathway terms that define specific types of infections or processes in the context of a particular disease were excluded.

After defining genomic loci, the association of all variants within GWAS loci (858 variants) with a set of clinical phenotypes in anti-GAD65 AINS patients was tested, namely the presence of a disease subtype (LE with TLS or TLE, CB with CA, SPS or any combination of these), comorbid T1DM, other autoimmune disorders or neoplasms, as well as high compared to low serum concentration of anti-GAD65 IgG (high: CBA ≥ 100 , ELISA ≥ 2000 U/ml, RIA ≥ 20 nmol/l)^{2,5,15} and absence compared to presence of intrathecal anti-GAD65 IgG synthesis. This analysis was adjusted for covariates as before but considered a nominal P -value ($P < 0.05$) to be suggestive of an association.

SNP heritability and LD score regression

We calculated the proportion of variance in sporadic anti-GAD65 AINS explained by our GWAS using the genome-based restricted

maximum likelihood (GREML)-LDMS (LD- and MAF-stratified GREML) method implemented in GCTA.^{16,17} For all autosomal variants in the imputed dataset, we calculated the 200 kb segment-based LD scores, stratified variants according to LD scores of individual SNPs, computed one genetic relationship matrix for each quartile of the stratified variants, and performed a restricted maximum likelihood analysis using these four matrices. The variance explained was estimated in a case-control setting, adjusting for covariates as before, and assuming a disease prevalence of 1.9/100 000 individuals.¹⁵ Additionally, to confirm that our findings were due to a polygenic architecture instead of batch effects, we calculated the LD score regression intercept using the LDSC software¹⁸ with LD scores pre-computed in 1000 Genomes European data, as suggested by the authors.

Analysis of the HLA region

In total, 6351 variants were extracted from the HLA region at chromosomal coordinates chr6:29–34 Mb. HLA allele genotypes for

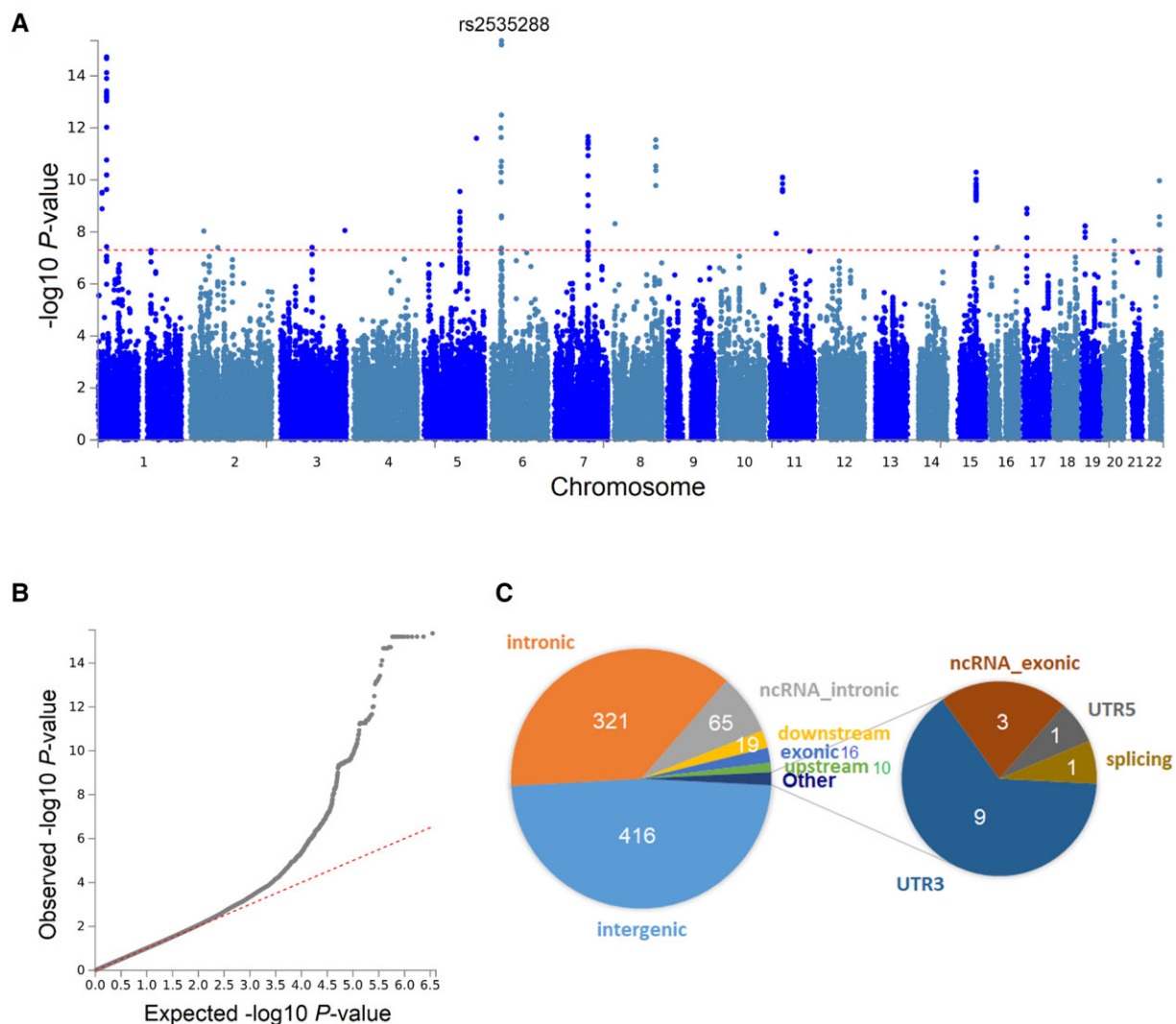


Figure 1 Overview of findings for the anti-GAD65 AINS GWAS. (A) Manhattan and (B) quantile-quantile plots of the anti-GAD65 AINS GWAS. The red dotted line in A depicts the threshold of genome-wide significance ($P < 5 \times 10^{-8}$). The total number of variants reaching this threshold was 191. The top variant was rs2535288 (chr6:31064007, $P = 4.42 \times 10^{-16}$, OR = 0.26, 95%CI = 0.187–0.358). (C) Functional consequences of all genome-wide and genomic loci variants in LD ($r^2 \geq 0.6$ and ± 500 kb from lead, $P < 0.05$). The greatest proportion of variants locates to intergenic and intronic regions of the genome.

the classical HLA class I loci HLA-A, -B, -C and class II loci HLA-DQA1, -DQB1, -DPB1 and -DRB1 were imputed using the Broad HLARES models for the Illumina Infinium Global Screening Array v2.0 using the R-package HLA genotype imputation without attribute bagging (HIBAG) (Version 1.20.0) at 4-digit resolution.¹⁹ We additionally imputed HLA nucleotides and amino acids, as well as performing HLA genotype phasing based on SHAPEIT2.^{20,21} A significance threshold of $P < 0.001$ was considered suggestive of an association for the purposes of our study.

Analysis of CSF proteome

To further substantiate the predictions on changes of protein expression levels in disease-relevant cells and tissues obtained from our GWAS, we added a CSF proteome study. We retrospectively identified a cohort of 10 patients with anti-GAD65 AINS, eight of whom were not part of the initial GWAS analysis, from our data base. The control group consisted of 10 age- and sex-matched patients with somatoform disorders. All participants gave written informed consent prior to sample acquisition and the study was approved by the ethics committee of the University of Muenster (2016-053-f-S and 2013-350-f-S). Liquid-chromatography ultra-high definition mass spectrometry (LC-UDMS) analysis was performed in 1 ml CSF. Complete methods can be found in the Supplementary material. The proteomics data was processed using Proteomics (Waters) and the Uniprot human database. Statistical analyses were additionally performed in R (<http://www.R-project.org/>). We compared groups with unpaired Mann–Whitney U-test. Volcano plots were created by plotting the log₂ fold change (LFC) of protein intensity values between both depicted experimental groups against their $-\log_{10} P$ -value. Significantly regulated proteins were defined as having a P -value of < 0.05 . The respective cut-offs are indicated as dotted lines.

Availability of data and materials

The datasets analysed in the current study are available from the authors on reasonable request. The results generated during this study are included in this published article and its supplementary information files.

Results

The initial study population included 205 anti-GAD65 AINS patients (62 males, 143 females) from the GENERATE network. After quality control and elimination of outliers and related individuals, 167 effective cases and 1047 controls remained. The cases consisted of 51 (31%) males versus 116 (69%) females, and the controls of 602 (57%) males and 445 (43%) females. In the anti-GAD65 AINS group, 101 (60%) patients had LE with TLS or TLE, 33 (20%) had CB with CA and 48 (29%) had SPS. An overlap syndrome was found in 17 (10%) patients, 39 (23%) patients had associated T1DM and 46 (28%) other autoimmune diseases, including autoimmune thyroid disease ($n = 34$; 20%), vitiligo ($n = 8$, 4.7%) and pernicious anaemia and/or autoimmune gastritis ($n = 6$, 3.5%) (for details, see Table 1).

No distortions of the observed or imputed genotypes due to independent genotyping of cases and controls were observed. There was good correlation of our dataset with the reference panel and of cases with control individuals (Supplementary Fig. 1). Our GWAS of anti-GAD65 AINS identified 191 associations at the genome-wide threshold of significance (Fig. 1A and B) and explained about 14.4% of the variance (h^2) on the liability scale. The genomic inflation factor, $\lambda = 1.026$, and the LD score regression intercept of 1.0037, corroborated that our findings were due to polygenicity. The top variant, rs2535288 [g.31064007C>A, $P = 4.42 \times 10^{-16}$, odds ratio (OR) = 0.26, MAF = 0.45, 95% confidence interval (CI) = 0.187–0.358], localizes to

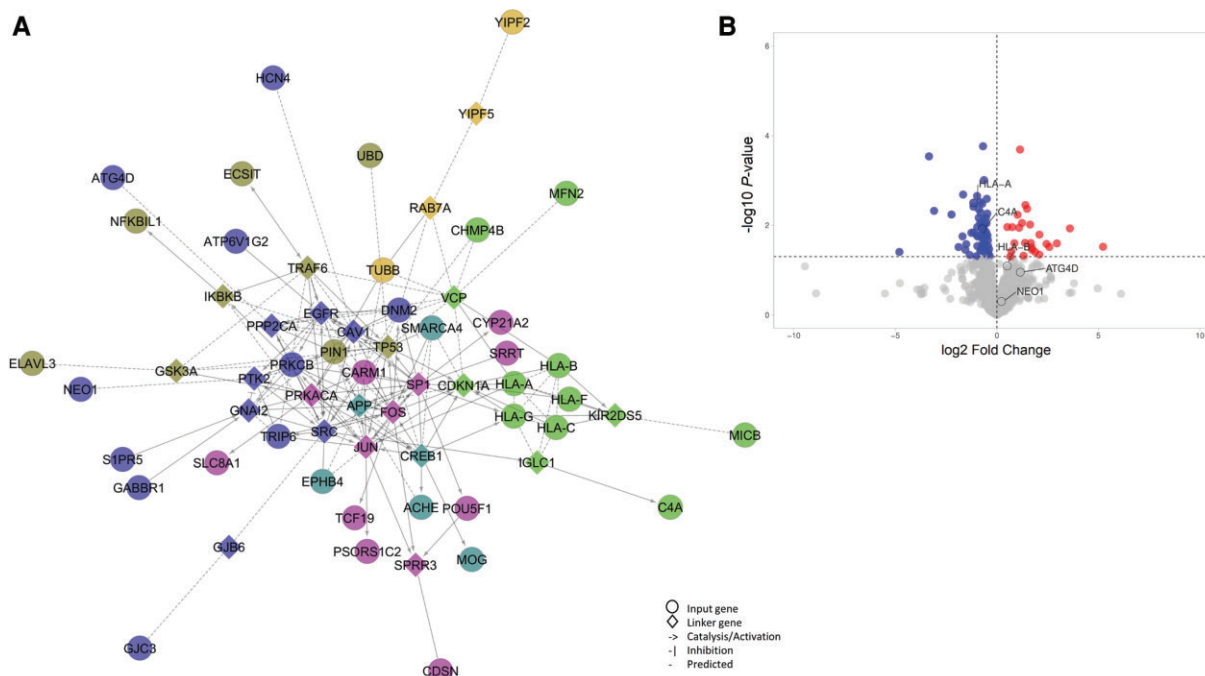


Figure 2 Investigation of GWAS findings at the protein level. (A) Protein-protein interaction network of GWAS coding genes. The network shows six functionally related gene clusters. Important connectors are SP1, FOS, TP53, JUN and SRC. (B) Volcano plot illustrating differential protein expression profiles in the CSF of anti-GAD65 AINS patients (red) compared to healthy controls (blue). HLA-A and C4A are differentially ($P < 0.05$) downregulated in anti-GAD65 AINS patients.

Table 2 Supported genomic loci for GAD65-AINS identified by our GWAS

| Locus | Index variant | Index alleles | Index location (bp) | Index P-value | Index OR | Chromosomal location | Start (bp) | End (bp) | Size (bp) | # Variants | # Ind.Sig. Variants | # Lead variants | Effects of variants | Mapped gene(s) |
|-------|---------------|---------------|---------------------|------------------------|----------|-----------------------|-------------|-------------|-----------|------------|---------------------|-----------------|---------------------|---|
| 1 | rs28718032 | T/C | 12 046 880 | 3.03×10^{-10} | 2.58 | chr1p36.22 | 12 046 089 | 12 068 546 | 22 457 | 6 | 1 | 1 | Risk | MFN2 |
| 2 | rs3091240 | T/G | 25 676 935 | 1.88×10^{-15} | 3.53 | chr1p36.11 | 25 663 071 | 25 851 977 | 188 906 | 31 | 2 | 1 | Risk + Protective | C1orf63; RP11-335G20.7; TMEM50A; RHCE; TMEM57/ MACO1; LDLRAP1 |
| 3 | rs11124749 | C/G | 40 821 576 | 9.29×10^{-9} | 2.27 | chr2p22.1 | 40 819 830 | 40 841 140 | 21 310 | 5 | 1 | 1 | Risk | SLC8A1 |
| 4 | rs2566748 | T/C | 82 292 908 | 3.99×10^{-8} | 2.19 | chr2p12 | 82 256 797 | 82 304 801 | 48 004 | 18 | 1 | 1 | Risk + Protective | ACO79896.1 |
| 5 | rs1822385 | C/A | 94 758 570 | 3.94×10^{-8} | 2.40 | chr3q11.2 | 94 749 987 | 94 760 796 | 10 809 | 4 | 1 | 1 | Risk | LINC00879 |
| 6 | rs6887291 | G/T | 106 438 742 | 2.78×10^{-10} | 0.35 | chr5q21.3 | 106 404 866 | 106 557 132 | 152 266 | 103 | 1 | 1 | Protective | CTC-254B4.1; PSMC1P5 |
| 7 | rs2535288 | C/A | 31 064 007 | 4.42×10^{-16} | 0.26 | chr6p21.33, chr6p22.1 | 29 488 249 | 31 105 310 | 1 617 061 | 244 | 10 | 3 | Risk + Protective | LINC01015; OR211P; UBD; GABBR1; MICG; HLA-W; MICD; HCG9; HCG17; TRIM26BP; PPP1R18; TUBE; MUC22; HCG22; RNU6-1133P; C6orf15; PSORS1C1; CDSN |
| 8 | rs314304 | G/A | 100 378 221 | 2.16×10^{-12} | 0.34 | chr7q22.1 | 100 368 671 | 100 523 241 | 154 570 | 113 | 3 | 1 | Mostly protective* | ZAN; EPHB4; SLC12A9; RP11-126L15.4; TRIP6; SRRT; UFSF1; ACHE; RN7SL549P; RP13-650G11.1 |
| 9 | rs12674939 | T/A | 126 479 907 | 2.87×10^{-12} | 2.84 | chr8q24.13 | 126 479 907 | 126 489 809 | 9902 | 16 | 1 | 1 | Risk | RP11-136012.2 |
| 10 | rs12806812 | A/G | 38 401 216 | 7.90×10^{-11} | 0.37 | chr11p12 | 38 400 126 | 38 429 604 | 29 478 | 18 | 1 | 1 | Mostly protective* | RP11-63D14.1 |

(continued)

Table 2 (continued)

| Locus | Index variant | Index alleles | Index location (bp) | Index P-value | Index OR | Chromosomal location | Start (bp) | End (bp) | Size (bp) | # Variants | # Ind.Sig. Variants | # Lead variants | Effects of variants | Mapped gene(s) |
|-------|---------------|---------------|---------------------|------------------------|----------|----------------------|------------|----------|-----------|------------|---------------------|-----------------|---------------------|----------------|
| 11 | 15:73543854 | C/C | 73543854 | 5.05×10^{-11} | 2.66 | chr15q24.1 | 73331183 | 73626970 | 295787 | 199 | 3 | 1 | Mostly risk* | NEO1, HCN4 |
| 12 | 16:24042219 | C/C | 24042219 | 3.92×10^{-8} | 0.43 | chr16p12.2 | 24042219 | 24053704 | 11485 | 5 | 1 | 1 | Risk + Protective | PRKCB |
| 13 | rs8082548 | G/A | 12418790 | 1.28×10^{-9} | 2.41 | chr17p12 | 12412583 | 12428515 | 15932 | 25 | 2 | 1 | Risk | LINC00670 |
| 14 | 19:10882215 | C/CT | 10882215 | 5.93×10^{-9} | 2.30 | chr19p13.2 | 10870866 | 10898413 | 27547 | 9 | 1 | 1 | Risk | DNM2 |
| 15 | rs2747537 | G/A | 32405217 | 2.19×10^{-8} | 2.32 | chr20q11.22 | 32399200 | 32470133 | 70933 | 16 | 1 | 1 | Risk + Protective | CHMP4B |
| 16 | rs62231498 | A/G | 44914879 | 1.08×10^{-10} | 3.53 | chr22q13.31 | 44888124 | 44926599 | 38475 | 45 | 2 | 2 | Risk + Protective | LDLOC1L |

bp = base pairs; Ind.Sig. = individually significant. *Most variants of the higher significance have these effects, although there are variants of lower significance with the opposite effects.

an intergenic genomic segment in the middle of the HLA class I region on chromosome 6. The variant exerts regulatory effects on multiple nearby genes (*HCG22*, *TCF19*, *HLA-B*) in brain tissue (frontal and temporal cortices) and immune cells (B cells and CD4⁺ T cells). It also shows various epigenetic marks (H3K4me1, H3K27me3, ZNF207 transcription factor) in brain cells (astrocytes, bipolar neurons), as well as in immune organs (thymus, spleen) and cells (T cells, CD14⁺ monocytes, common myeloid progenitors). Moreover, diverse genome-wide variants in LD with rs2535288 supported this association signal.

According to the applied criteria (see ‘Methods’ section), 16 genomic loci for anti-GAD65 AINS were defined by the combination of our GWAS summary statistics and LD information (Supplementary Figs 2–17). In total, these genomic loci contained 858 variants, of which 32 were independently significant, and 19 were lead variants, mapping to 48 genes in total (Table 2). All genome-wide and loci variants (including those genome-wide variants that were excluded from further analysis due to a lack of signal support) are listed in Supplementary Table 2. In their majority, these variants were intergenic (48.3%) or localized to introns of coding (37.3%) and non-coding (7.6%) genes (Fig. 1C). The annotation of variants in genomic loci showed that 358 variants have 1972 associations with the expression levels of 47 genes, including 39 non-mapped genes, in the brain (preferentially frontal cortex) and immune cell types (preferentially CD4⁺ T cells) from the BRAINEAC and DICE eQTL datasets. This suggests that the regulation of gene expression in disease relevant cells and tissues is one of the molecular mechanisms by which the identified associations contribute to the pathobiology of anti-GAD65 AINS (for the genomic locus context of these eQTL annotations see Supplementary Table 3 and Supplementary Figs 2–17).

In addition, over 6000 annotations from the Roadmap and ENCODE epigenomics datasets that were obtained for 728 variants in the GWAS genomic loci gave insights into cell type and tissue specificity. The most frequent epigenomes encountered were neuronal cells (including neural stem progenitor cells) and immune cells (including CD14⁺ monocytes, CD34⁺ common myeloid progenitors and T cells). The most frequent epigenetic marks were the histone modifications H3K4me1, H3K36me3 and H3K27me3 (Table 3). Epigenetic annotations specific for each GWAS locus are presented in Supplementary Table 4.

The most significant and largest locus (#7), located in the HLA class I region, harboured 244 variants with both risk and protective effects, of which 10 were independent signals and three were lead variants. Eighteen genes mapped to this locus (Table 2). In addition, variants within this locus have been reported as eQTLs in brain and/or immune cells of 21 non-mapped genes. Of note, five eQTL genes (*HLA-F*, *HCG18*, *MICB*, *C4A*, *VARS2*) were found exclusively in the brain dataset, while *HCG22* showed the largest numbers of eQTLs in both the BRAINEAC (149 eQTLs in the average of all regions) and DICE (23 eQTLs in naïve B cells) datasets (Supplementary Table 3). Expectedly, epigenetic marks, particularly H3K4me1, were more common in epigenomes of diverse immune cells, most prominently of common myeloid progenitors.

The second (locus #2, chromosome 1, index variant: rs3091240, $P = 1.88 \times 10^{-15}$, OR = 3.53, 95%CI = 2.587–4.819) and third (locus #8, chromosome 7, index variant: rs314304, $P = 2.16 \times 10^{-12}$, OR = 0.34, 95%CI = 0.254–0.461) most significant loci mapped to more than two genes (Table 2). Mapped and eQTL genes in these loci implicated the Rh blood group cluster (*RHCE*, *RHD*, *TMEM50A*) and genes with important functions in neuronal development and function (*MACO1*, *ACHE*, *TRIP6*, *SRRT*, *EPHB4*) in the biology of anti-GAD65

Table 3 Summary of epigenetic marks annotated for variants in GWAS loci

| Feature | Database | n | % |
|---|----------|------|-------|
| Epigenome: cell types | | | |
| Bipolar neuron | ENCODE | 825 | 13.42 |
| Neuron | Roadmap | 279 | 4.54 |
| Monocytes-CD14+ | ENCODE | 511 | 8.31 |
| CD14 positive monocyte | ENCODE | 413 | 6.72 |
| Monocytes-CD14+ (peripheral blood) | Roadmap | 305 | 4.96 |
| Common myeloid progenitor CD34 positive (ENCSR337XXD 1) | Roadmap | 434 | 7.06 |
| Common myeloid progenitor CD34 positive | Roadmap | 350 | 5.69 |
| Common myeloid progenitor CD34 positive (ENCSR722JRY) | Roadmap | 141 | 2.29 |
| Neural stem progenitor cell | Roadmap | 431 | 7.01 |
| Neural progenitor cell | ENCODE | 88 | 1.43 |
| T cells (peripheral blood) | Roadmap | 386 | 6.28 |
| T cell | Roadmap | 13 | 0.21 |
| T helper 17 cell | Roadmap | 104 | 1.69 |
| Neutrophil | Roadmap | 181 | 2.94 |
| B cells (peripheral blood) | Roadmap | 176 | 2.86 |
| B cell (ENCSR682AXR) | ENCODE | 126 | 2.05 |
| B cell | Roadmap | 16 | 0.26 |
| B cell (ENCSR241CUA 1) | Roadmap | 14 | 0.23 |
| Natural Killer cells (peripheral blood) | Roadmap | 171 | 2.78 |
| CD4 positive alpha beta T cell (ENCSR948ZKZ) | Roadmap | 145 | 2.36 |
| CD4 positive alpha beta T cell | Roadmap | 134 | 2.18 |
| CD4 positive CD25 positive alpha beta regulatory T cell | Roadmap | 104 | 1.69 |
| Naive thymus derived CD4 positive alpha beta T cell | Roadmap | 90 | 1.46 |
| CD4 positive alpha beta memory T cell | Roadmap | 55 | 0.89 |
| Effector memory CD4 positive alpha beta T cell | Roadmap | 17 | 0.28 |
| Astrocyte | ENCODE | 111 | 1.81 |
| Astrocyte (ENCSR362MQF) | ENCODE | 14 | 0.23 |
| Astrocyte (ENCSR362MQF 1) | ENCODE | 12 | 0.20 |
| Cardiac muscle cell | ENCODE | 84 | 1.37 |
| Epigenome: organs | | | |
| Spleen | Roadmap | 186 | 3.03 |
| Heart | Roadmap | 110 | 1.79 |
| Brain | Roadmap | 106 | 1.72 |
| Brain (ENCSR189GMC-female embryo) | Roadmap | 15 | 0.24 |
| Marker | | | |
| H3K4me1 (histone) | Both | 1780 | 28.96 |
| H3K36me3 (histone) | Both | 1479 | 24.06 |
| H3K27me3 (histone) | Both | 1376 | 22.38 |
| H3K9me3 (histone) | Both | 435 | 7.08 |
| H3K27ac (histone) | Both | 344 | 5.60 |
| H3K4me3 (histone) | Both | 262 | 4.26 |
| DNase1 (open chromatin) | Both | 206 | 3.35 |
| CTCF (transcription factor) | Both | 177 | 2.88 |
| H4K20me1 (histone) | Both | 54 | 0.88 |
| H3K4me2 (histone) | Both | 19 | 0.31 |
| H3K9ac (histone) | Both | 11 | 0.18 |
| EZH2 (transcription factor) | Both | 4 | 0.07 |

AINS. The majority of the identified loci mapped to only one protein-coding or non-coding gene (10/16) and contained variants with both, risk and protective effects (9/16). However, three of the 'mixed effects' loci might be assumed to have either mostly protective (loci #8 and 10) or mostly risk (#11) effects on the anti-GAD65 AINS phenotype, driven by the variants of highest significance

within the locus. Six loci contained only risk variants, while one contained only variants with protective effects (locus #6). The biological implications of some of these loci are not clear from our analyses, not only because they mapped to non-coding genes, but also because no eQTL effects for these variants were found in the relevant datasets.

For the protein-coding genes that physically mapped to our anti-GAD65 AINS GWAS loci and/or are regulated by these variants (i.e. eQTL genes) in the relevant datasets, we created a PPI network to provide some biological context for our findings beyond the immune component driven by the HLA. The resulting network comprised 62 genes, of which 38 were GWAS input and 24 as linker genes (Fig. 2A). Unsurprisingly, the largest number of functional interactions in the network was observed for linker genes. These network hubs included TP53, FOS and SP1, with 18 interactions each, as well as JUN and SRC, with 17 interactions each. From the input genes, the most largely connected node was protein kinase C beta (PRKCB) from the GWAS locus #12, with 13 interactions. The clustering of the network defined six modules, with 17 genes in the largest and four genes in the smallest module (Table 4). In total, 115 module pathway enrichments passed our criteria (Supplementary Table 5). These included 85 unique pathway terms, with overlaps observed mainly between modules #0 (lilac) and #2 (magenta), including various cell signalling pathways related to immunity and neural function. As expected, all network modules were highly enriched in signalling pathways that relate to immunity, including antigen presentation and autoimmunity, which concentrated in the module #1 (green), as well as innate immune pathways, such as the Toll-like and RIG-I-like receptor cascades. Enrichment was found in signalling pathways of other molecules and activation of receptors, whose functions might not primarily be immune, but have known roles in immune regulation. These included lysophosphatidic acid (LPA) receptors, sphingolipids, oestrogen, oxytocin, gonadotropin-releasing hormone (GnRH) and relaxin (Supplementary Table 5).

In addition, a total of 411 associations with all nine clinical variables were found at the nominal level for 290 anti-GAD65 AINS loci variants. These highlighted the importance of locus #7 for almost all of the phenotypes tested (with the exception of the overlapping of LE/SPS/CB), but particularly for LE with TLS/TLE, T1DM and intra-thecal synthesis, for which the lowest P-values were found in this GWAS locus (Table 5). Our results suggest that both loci #7 and #8 overlap between different types of anti-GAD65 AINS, as well as other autoimmune diseases and the presence of a neoplasm. Differences between these might be influenced by variants in other loci, particularly in loci #5, #6, #10 and #11. Interestingly, loci #5 and #11, which together showed associations with SPS and the presence of a neoplasm, have risk effects, while loci #6 and #10, which appear to influence CB, showed protective effects in our GWAS. This illustrates how variations in multiple regions of the genome and their interactions contribute to distinctive phenotypes.

Our analysis of the HLA classical alleles and haplotypes showed no associations at the genome-wide level and no overlaps with the GWAS genome-wide signals in the region (Fig. 3A). Nonetheless, because only a segment of the genome is tested in this analysis and considering the relatively small sample size of our study, we chose to lower the threshold for suggestive associations to $P < 0.001$. At this threshold, one significant haplotype (DQA1*03:01-DQB1*03:02-DRB1*04:01, $P = 4.29 \times 10^{-4}$, OR = 2.5, frequency = 0.064, 95%CI = 1.499–4.157) and one significant allele (DRB1*04:01, $P = 8.3 \times 10^{-5}$, OR = 2.39, frequency = 0.094, 95%CI = 1.548–3.682) conferring risk for anti-GAD65 AINS were found, together with two significant

Table 4 Summary of network modules

| Module | Color | Nodes | Genes | Pathways | Top three pathways | Summary pathway class(es) |
|--------|---------|-------|---|----------|--|--|
| 0 | Lilac | 17 | ATG4D , ATP6V1G2 , CAV1 , DNM2 , EGFR , GABBR1 , GJB6 , GJC3 , GNAI2 , HCN4 , NEO1 , PPP2CA , PRKCB , PTK2 , S1PR5 , SRC , TRIP6 | 49 | Signalling events mediated by VEGFR1 and VEGFR2, LPA receptor mediated events, Thromboxane A2 receptor signalling | Cell signalling mediating immune and neuronal processes |
| 1 | Green | 13 | C4A , CDKN1A , CHMP4B , HLA-A , HLA-B , HLA-C , HLA-F , HLA-G , IGLC1 , KIR2DS5 , MFN2 , MICB , VCP | 16 | Antigen processing and presentation, Allograft rejection, Immunoregulatory interactions between a lymphoid and a non-lymphoid cell | Antigen processing and presentation, Autoimmunity, interferon signalling |
| 2 | Magenta | 13 | CARM1 , CDSN , CYP21A2 , FOS , JUN , POU5F1 , PRKACA , PSORS1C2 , SLC8A1 , SP1 , SPRR3 , SRRT , TCF19 | 30 | ESR-mediated signalling, Calcium signalling in the CD4+ TCR pathway, ErbB2/ErbB3 signalling events | Cell signalling mediating immune and neuronal processes |
| 3 | Olive | 9 | ECSIT , ELAVL3 , GSK3A , IKBKB , NFKBIL1 , PIN1 , TP53 , TRAF6 , UBD | 11 | Toll-like receptor pathway, Signal transduction through IL1R, p75(NTR)-mediated signalling | Inflammation, neurotrophin signalling |
| 4 | Aqua | 6 | ACHE , APP , CREB1 , EPHB4 , MOG , SMARCA4 | 7 | ATF-2 transcription factor network, Glucocorticoid receptor regulatory network, Cholinergic synapse | Macrophage activity |
| 5 | Mustard | 4 | RAB7A , TUBB , YIPF2 , YIPF5 | 2 | Phagosome, Neutrophil degranulation | Innate immunity |

Input genes for the network are highlighted in bold.

amino acids and three significant nucleotides conferring protection (Table 6 and Fig. 3B). The most common suggestive protective and risk HLA haplotypes in our cohort were DQA1*05:05-DQB1*03:01 (OR = 0.45, frequency = 0.1223, 95%CI = 0.264–0.759) and DQA1*05:01-DQB1*02:01-DRB1*03:01 (OR = 2.02, frequency = 0.121, 95%CI = 1.223–3.329), respectively.

Finally, we identified five proteins (HLA-A/B, C4A, ATG4D and NEO1) of eQTL genes from our GWAS in the CSF proteome of anti-GAD65 AINS patients (Fig 2B, clinical data in Table 1). Moreover, compared to controls, these changes were consistent with the effect direction in immune cells for the corresponding gene annotated from DICE in our GWAS, including elevation of HLA-B (B cells) and NEO1 (B and T cells) as well as decrease in HLA-A (T cells). HLA-A ($P=0.003$, $LFC=-1.14$) and C4A ($P=0.012$, $LFC=-0.72$) showed differential levels in patients.

Discussion

We conducted a GWAS of sporadic anti-GAD65 AINS in a cohort of 167 patients and over 1000 population-based controls. The demographic characteristics of our study population are in line with previous studies regarding sex and age, as well as the distribution of clinical phenotypes.^{2,3,6} The presence of overlapping clinical phenotypes in 10% of our patients underlines the view of anti-GAD65 AINS as a disease spectrum rather than separate disease entities, similar to what has been previously described.² We focused our inclusion on a typical clinical phenotype, confirmed by a typical staining pattern in a TBA on rodent or non-human primate brain (and pancreas), which is indicative of high autoantibody titres.³ We included patients who fulfilled these criteria, even if they had 'low' titres in the tertiary quantitative analyses, to study the full spectrum of anti-GAD65 AINS.

Our GWAS identified 16 genomic loci for anti-GAD65 AINS at the genome-wide threshold of significance. These included mainly

intergenic or intronic variants outside the classic HLA genomic region. The annotation of these variants with eQTL and epigenetic datasets, as well as the network analysis of the implicated protein-coding genes, consistently underscored variations in both CNS tissues and immune cells. T-cell infiltrates have been detected in close spatial proximity to neurons of the hippocampus in anti-GAD65 TLE,²² genetic variations resulting in altered interaction between the immune cells and the neurons could facilitate this.

Our PPI network analysis further illustrated the complex interplay of immune and neural signalling pathways relevant for anti-GAD65 AINS pathophysiology. According to the information contained in the GWAS Catalog,²³ several of the non-classical HLA genes implicated in anti-GAD65 AINS by our study have known associations with the susceptibility to different autoimmune disorders, such as T1DM, multiple sclerosis, psoriasis, arthritis and Crohn's disease. Among these genes are EPHB4, PRKCB and SMARCA4. The most common associated autoimmune diseases in our sample besides T1DM, were autoimmune thyroid diseases and vitiligo, for which some genetic susceptibility traits overlapping with genetic variations in anti-GAD65 AINS have been reported.^{6,24–27}

Previous genetic studies of anti-GAD65 AINS have focused on the HLA class II region, suggesting associations in both familial and sporadic cases.^{4–6} Our study did not find associations in this genomic locus at the genome-wide level of significance, neither in our GWAS, nor the HLA association analysis. Therefore, we lowered the significance threshold to consider an HLA-association 'suggestive' and searched for the most common haplotypes, based on their frequencies in our cohort. Thereby we were able to detect one haplotype and one allele in the HLA class II genomic locus that might contribute to the risk for anti-GAD65 AINS in our cohort. The suggested haplotype, DQA1*03:01-DQB1*03:02-DRB1*04:01, has been identified as one of the susceptibility haplotypes for T1DM,²⁸ with DQB1*03:02 reported as one of the high-risk alleles,²⁹ while

Table 5 Summary of associations of variants in GWAS loci with clinical phenotypes

| Clinical phenotype | Total cases | Effective cases | Nominal associations | GWAS loci ^a |
|---|-------------|-----------------|----------------------|------------------------|
| Limbic encephalitis | 125 | 101 | 58 | 7,8,11 |
| Stiff-person syndrome | 57 | 48 | 63 | 5,7,8,11 |
| Cerebellitis | 36 | 33 | 28 | 6,7,8,10 |
| Any combination of the above | 20 | 17 | 25 | 9,11,12,13 |
| Type 1 diabetes mellitus (T1DM) | 41 | 39 | 40 | 2,4,7,8,9,10 |
| Autoimmune disorders other than T1DM | 53 | 46 | 66 | 7,8,10 |
| Presence of neoplasm | 19 | 15 | 14 | 5,7,8,11,15 |
| Anti-GAD65 IgG concentration (CBA: 1/Titre, ELISA: U/ml, RIA: nmol/l) in serum. High (CBA ≥ 100, ELISA ≥ 2000 U/ml, RIA ≥ 20 nmol/l) | 149 | 120 | 98 | 4,7,14,16 |
| Intrathecal synthesis (with method-based cut off CBA/TBA 4, ELISA/RIA 1.5) | 140 | 123 | 19 | 7,11,15 |

^aThe locus showing the lowest P-values is highlighted in bold.

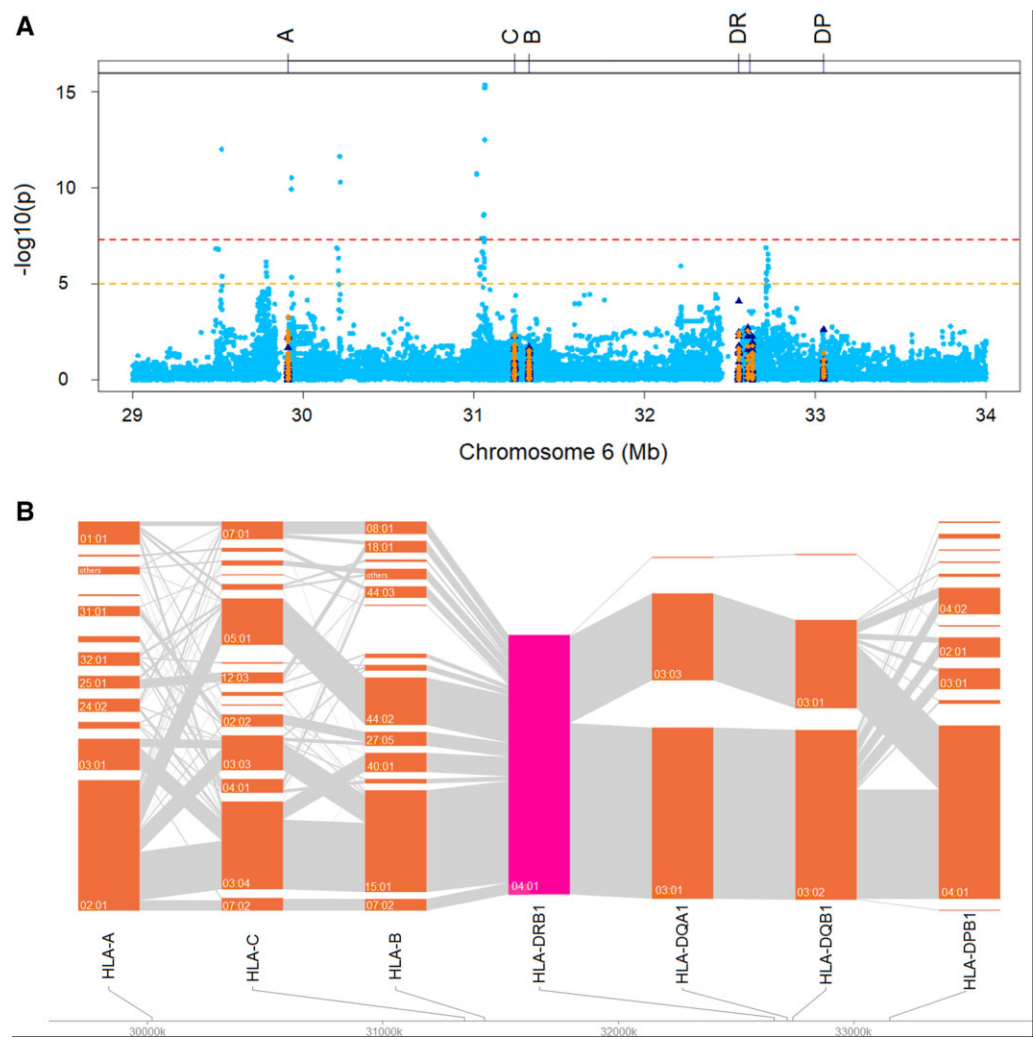


Figure 3 Analysis of the classical HLA alleles and haplotypes. (A) Manhattan and (B) disentangler plots of the analysis of the classical HLA alleles and haplotypes. In A, the GWAS variants are shown in light blue, the classical alleles in dark blue and the amino acid variants in orange. The yellow and red dotted lines indicate the commonly used suggestive ($P < 1 \times 10^{-5}$) and genome-wide ($P < 5 \times 10^{-8}$) significance thresholds, respectively. In B, the relationships of the allele of highest significance in our study, HLA-DRB1*04:01, with other classical alleles in the whole GWAS dataset are shown as disentangler plot.³⁶

our study defined this as DRB1*04:01 for anti-GAD65 AINS. In our cohort, 39 patients had an associated T1DM, out of which only 10 carried the DQA1*03:01-DQB1*03:02-DRB1*04:01 haplotype. This haplotype was also present in 17 cases that did not have T1DM, and vice versa, 26 cases had an associated T1DM but carried other HLA haplotypes. This haplotype has been reported as a genetic

Table 6 HLA region findings at the threshold $P < 0.001$

| Type | Feature | Position | Effect | Non effect | n | P | OR | 95% CI | Frequency |
|---|---|----------|--------|------------|------|-----------------------|-----------------------|-------------------------------|-----------|
| Suggestive threshold ($P < 0.001$) | | | | | | | | | |
| Haplotype | DQA1*03:01-DQB1*03:02-DRB1*04:01 | - | P | A | 1091 | 4.39×10^{-4} | 2.496 | 1.499–4.157 | 0.0637 |
| Allele | imputed_HLA_DRB1*04:01 | 32552086 | P | A | 1214 | 8.30×10^{-5} | 2.387 | 1.548–3.682 | 0.09432 |
| Amino acid | imputed_prot_A_166 | 166 | D | E | 1214 | 5.41×10^{-4} | 0.4872 | 0.324–0.732 | 0.2801 |
| Amino acid | imputed_prot_A_167 | 167 | G | W | 1214 | 5.41×10^{-4} | 0.4872 | 0.324–0.732 | 0.2801 |
| Nucleotide | imputed_nuc_A_29910761 | 29910761 | A | G | 1214 | 3.02×10^{-5} | 0.498 | 0.359–0.691 | 0.3904 |
| Nucleotide | imputed_nuc_A_29911271 | 29911271 | C | G | 1214 | 5.41×10^{-4} | 0.4872 | 0.324–0.732 | 0.2801 |
| Nucleotide | imputed_nuc_A_29911272 | 29911272 | G | T | 1214 | 5.41×10^{-4} | 0.4872 | 0.324–0.732 | 0.2801 |
| Other haplotypes of interest | | | | | | | | | |
| Haplotype | DQA1*05:05-DQB1*03:01 | - | P | A | 1108 | 2.84×10^{-3} | 0.4477 | 0.264–0.759 | 0.1223 |
| Haplotype | DPB1*04:01-DQA1*01:03-DQB1*06:03-A*02:01-C*05:01-DRB1*13:01-B*44:02 | - | P | A | 941 | 2.94×10^{-3} | 17.38 | 2.647–114.1 | 0.002657 |
| Haplotype | DQA1*05:01-DQB1*02:01 | - | P | A | 1108 | 5.14×10^{-3} | 2.042 | 1.238–3.368 | 0.1196 |
| Haplotype | DQA1*05:01-DQB1*02:01-DRB1*03:01 | - | P | A | 1091 | 6.00×10^{-3} | 2.018 | 1.223–3.329 | 0.121 |
| Haplotype | A*31:01-C*04:01-B*35:01 | - | P | A | 1168 | 8.36×10^{-3} | 4.71×10^{-4} | 1.59×10^{-5} –0.1399 | 0.0008562 |
| Haplotype | DPB1*04:01-DQA1*02:01-DQB1*02:02-A*01:01-C*07:01-DRB1*07:01-B*08:01 | - | P | A | 941 | 8.70×10^{-3} | 45.24 | 2.623–780.3 | 0.001063 |

risk factor in polyglandular autoimmune syndrome type 2.³⁰ The DRB1*04:01 allele as such has been reported in association with T1DM and rheumatoid arthritis.^{31,32} Furthermore, it plays a role in the interaction of multiple sclerosis and other autoimmune diseases,³³ which supports the hypothesis that different autoimmune diseases share a genetic risk.³⁴

Additionally, the most common HLA class II risk haplotype identified in our study (DQA1*05:01-DQB1*02:01-DRB1*03:01), was reported as the most frequent haplotype in a previous association study of the HLA in 32 anti-GAD65 patients.⁴

We assessed whether our GWAS signals were specific for particular anti-GAD65 AINS phenotype and, although we did not find any genome-wide significant associations, we observed about 400 associations at the nominal level of significance. Associations with the most prominent loci (locus #7 and #8), which mapped to both immune-related genes, including the HLA class I region, and to neural-related genes, including inhibitory neuronal signalling and neuronal structure and development, were present across all phenotypes (but not their combinations). There were subtle associations in loci #5, #6, #10 and #11, which could point towards a difference in genetic vulnerability for a certain phenotype. It is conceivable, that many subtle genetic signals with particular anti-GAD65 AINS phenotypes were lost in our study due to the small sample size when dividing into subgroups. Particular genetic loci might interact with each other, exerting a cumulative effect. Downstream effects (i.e. post-transcriptional and post-translational modifications) could explain differences among phenotypes. Additionally, our study did not take into consideration the effects of external factors, such as the living situation, exposure to different environments or preceding infections, which could have influenced the development of anti-GAD65 AINS, similar to what has been suggested for T1DM and Hashimoto's disease.³⁵ As this was not the main concern of the present work, it should be the focus of further studies. Another task for further studies will be translating the results to therapeutic strategies, since traditional immunosuppression has limited effects.³ Our protein-protein interaction network highlighted the importance of PRKCB, a factor in cell death and cell survival, and SMARCA4 which is reported to be involved in the regulation of neural stem cell renewal and proliferation (GWAS Catalogue),²³ which may be potential targets for neuroprotective strategies.

There are other limitations to our study: Due to the rarity of the disease, we worked with a German, strictly Caucasian sample, which could have influenced the results. In the future, an international sample could provide further insights into the genetic architecture of anti-GAD65 AINS. Moreover, we acknowledge that focusing on common variants might result in the effect of important yet rare genetic variants being missed while the effects of the most common variants might be overestimated. We tried to overcome some of these limitations by applying stringent QC and performing an array of downstream analyses, including investigation in proteomics data from the CSF. Although our proteomics sample is still small, we believe the observed overlaps with our GWAS findings are encouraging.

In conclusion, we demonstrated that common variations at numerous genes involved in innate and adaptive immunity, as well as contributing to neural structure and function, modulate the susceptibility to anti-GAD65 AINS. The implicated protein-coding genes are part of a network of biological pathways with various cross-links between the CNS development and function and immunity. Although the most significant locus was located in the HLA class I region, classical HLA analysis could only point to

potential haplotype associations located to the HLA class II region. Our findings highlighted the involvement of different immune cell types and the brain itself in the pathogenesis of anti-GAD65 AINS. In individuals with a predisposition to aberrant immune responses and altered neuronal structure and function, a bidirectional interaction could explain the poor treatment response, which warrants a deeper analysis of the cause-and-effect relationship in anti-GAD65 AINS and other neurological disorders.

Acknowledgements

We are indebted to all patients and their relatives, and to all members of the GENERATE network (www.generate-net.de) for supporting this study through patient recruitment, data acquisition and entry. All authors and contributing members of the GENERATE network as of July 2021 as well as all other contributors are indicated in [Supplementary Table 1](#).

Funding

This project was supported by the German Research Foundation (ERARE18-202 UltraAIE) under the frame of E-Rare-3, the ERA-Net for Research on Rare Diseases, the German Federal Ministry of Education and Research (Comprehensive, Orchestrated, National Network to Explain, Categorize and Treat autoimmune encephalitis and allied diseases within the German Network for Research on Autoimmune Encephalitis – CONNECT GENERATE; 01GM1908), and the Innovative Medizinische Forschung Münster, Germany (IMF; ST 212006).

Competing interests

The authors declare no competing interests.

Supplementary material

[Supplementary material](#) is available at *Brain* online.

Appendix 1

Members of the German Network for Research on Autoimmune Encephalitis (GENERATE)

For institutions and contact information, please refer to the [Supplementary material](#).

Michael Adelman, Luise Appeltshauser, Ilya Ayzenberg, Carolin Baade-Büttner, Andreas van Baalen, Sebastian Baatz, Bettina Balint, Sebastian Bauer, Annette Baumgartner, Sonka Benesch, Robert Berger, Sascha Berning, Sarah Bernsen, Christian Bien, Corinna Bien, Andreas Binder, Stefan Bittner, Daniel Bittner, Franz Blaes, Astrid Blaschek, Justina Dargvainiene, Julia Decker, Andre Dik, Kathrin Doppler, Mona Dreesmann, Friedrich Ebinger, Lena Edelhoff, Sven Ehrlich, Katharina Eisenhut, Dominique Endres, Marina Entschewa, Jürgen Hartmut Faiss, Kim Kristin Falk, Walid Fazeli, Alexander Finke, Carsten Finke, Dirk Fitzner, Marina Flotats-Bastardas, Mathias Fousse, Paul Friedemann, Manuel Frieze, Marco Gallus, Marcel Gebhard, Christian Geis, Clemens Goedel, Anna Gorsler, Armin Grau, Oliver Grauer, Catharina Groß, Halime Gül, Chung, Ha-Yeun, Aiden Haghikia, Robert Handreka, Niels Hansen, Martin Häusler, Joachim Havla, Wolfgang Heide, Valentin Held, Kerstin Hellwig, Philip Hillebrand, Frank Hoffmann,

Anna Hoffmann, Ulrich Hofstadt-van Oy, Peter Huppke, Fatme Seval Ismail, Martina Jansen, Aleksandra Juranek, Michael Karenfort, Max Kaufmann, Christoph Kellinghaus, Constanze Kerin (Mönig), Susanne Knake, Peter Körtvéyessy, Stjepana Kovac, Andrea Kraft, Markus Krämer, Christos Krogias, Tanja Kümpfel, Christoph Lechrich, Jan Lewerenz, Frank Leypoldt, Andreas Lins, Jan Lünemann, Michael Malter, Monika Meister, Nico Melzer, Kristin Stefanie Melzer (Golombeck), Til Menge, Sven Meuth, Gerd Meyer zu Hörste, Marie-Luise Mono, Sigrid Mues, Michael Nagel, Christopher Nelke, Tobias Neumann-Haefelin, Jost Obrocki, Loana Penner, Lena Kristina Pfeffer, Thomas Pfefferkorn, Alexandra Philippsen, Johannes Piepgras, Felix von Poderwils, Josef Priller, Anne-Katrin Probstel, Harald Prüß, Johanna Maria Helena Rau, Saskia Jania Räuber, Gernot Reimann, Raphael Reinecke, Marius Ringelstein, Hendrik Rohner, Felix Rosenow, Kevin Rostasy, Theodor Rüber, Stephan Rüegg, Jens Schaumberg, Ruth Schilling, Mareike Schimmel, Jens Schmidt, Ina-Isabelle Schmütz, Stephan Schreiber, Gesa Schreyer, Ina Schröder, Christina Schröter, Simon Schuster, Günter Seidel, Makbule Senel, Kai Siebenbrodt, Claudia Sommer, Oliver Stammel, Martin Stangel, Henning Stolze, Muriel Stoppe, Karin Storm van's Gravesande, Christine Strippel, Dietrich Sturm, Kurt-Wolfram Sühs, Steffen Syrbe, Simone Tauber, Malte Teußer, Franziska Thaler, Florian Then Bergh, Corinna Trebst, George Trendelenburg, Regina Trollmann, Hayrettin Tuman, Methab Türedi, Christian Urbanek, Niklas Vogel, Matthias von Mering, Judith Wagner, Klaus-Peter Wandinger, Robert Weissert, Jonathan Wickel, Heinz Wiendl, Brigitte Wildemann, Karsten Witt, Benjamin Wunderlich, Lara Zieger.

References

1. Graus F, Titulaer MJ, Balu R, et al. A clinical approach to diagnosis of autoimmune encephalitis. *Lancet Neurol*. 2016;15(4):391–404.
2. Saiz A, Blanco Y, Sabater L, et al. Spectrum of neurological syndromes associated with glutamic acid decarboxylase antibodies: Diagnostic clues for this association. *Brain*. 2008;131(10):2553–2563.
3. Muñoz-Lopetegi A, de Bruijn MAAM, Boukhrissi S, et al. Neurologic syndromes related to anti-GAD65: Clinical and serologic response to treatment. *Neurol Neuroimmunol Neuroinflamm*. 2020;7(3):e696.
4. Muñoz-Castrillo S, Ambati A, Dubois V, et al. Primary DQ effect in the association between HLA and neurological syndromes with anti-GAD65 antibodies. *J Neurol*. 2020;267(7):1906–1911.
5. Belbezier A, Joubert B, Montero-Martin G, et al. Multiplex family with GAD65-Abs neurologic syndromes. *Neurol Neuroimmunol Neuroinflamm*. 2017;5(1):e416–e416.
6. Thaler FS, Bangol B, Biljecki M, Havla J, Schumacher A-M, Kümpfel T. Possible link of genetic variants to autoimmunity in GAD-antibody-associated neurological disorders. *J Neurol Sci*. 2020;413:116860.
7. Reiber H, Peter JB. Cerebrospinal fluid analysis: disease-related data patterns and evaluation programs. *J Neurol Sci*. 2001;184(2):101–122.
8. Nöthlings U, Krawczak M. PopGen: Eine populationsbasierte Biobank mit Langzeitverfolgung der Kontrollkohorte. *Bundesgesundheitsblatt Gesundheitsforsch Gesundheitsschutz*. 2012;55(6–7):831–835.
9. Das S, Forer L, Schönherr S, et al. Next-generation genotype imputation service and methods. *Nat Genet*. 2016;48(10):1284–1287.

10. Chang CC, Chow CC, Tellier LC, Vattikuti S, Purcell SM, Lee JJ. Second-generation PLINK: rising to the challenge of larger and richer datasets. *Gigascience*. 2015;4:7.
11. Watanabe K, Taskesen E, Van Bochoven A, Posthuma D. Functional mapping and annotation of genetic associations with FUMA. *Nat Commun*. 2017;8(1):1–10.
12. Oscanoa J, Sivapalan L, Gadaleta E, Dayem Ullah AZ, Lemoine NR, Chelala C. SNPnexus: A web server for functional annotation of human genome sequence variation (2020 update). *Nucleic Acids Res*. 2020;48(W1):W185–W192.
13. Shannon P, Markiel A, Ozier O, et al. Cytoscape: A software environment for integrated models. *Genome Res*. 2003;13(11):426.
14. Wu G, Dawson E, Duong A, Haw R, Stein L. ReactomeFIViz: A cytoscape app for pathway and network-based data analysis. *F1000Research*. 2014;3:1–15.
15. Dubey D, Pittock SJ, Kelly CR, et al. Autoimmune encephalitis epidemiology and a comparison to infectious encephalitis. *Ann Neurol*. 2018;83(1):166–177.
16. Yang J, Lee SH, Goddard ME, Visscher PM. GCTA: A tool for genome-wide complex trait analysis. *Am J Hum Genet*. 2011;88(1):76–82.
17. Yang J, Bakshi A, Zhu Z, et al. Genetic variance estimation with imputed variants finds negligible missing heritability for human height and body mass index. *Nat Genet*. 2015;47(10):1114–1120.
18. Bulik-Sullivan BK, Neale BM. LD score regression distinguishes confounding from polygenicity in GWAS. *Nat Genet*. 2015;47(3):291–295.
19. Zheng X, Shen J, Cox C, et al. HIBAG - HLA genotype imputation with attribute bagging. *Pharmacogenomics J*. 2014;14(2):192–200.
20. Delaneau O, Zagury JF, Marchini J. Improved whole-chromosome phasing for disease and population genetic studies. *Nat Methods*. 2013;10(1):5–6.
21. Degenhardt F, Mayr G, Wendorff M, et al. Transethnic analysis of the human leukocyte antigen region for ulcerative colitis reveals not only shared but also ethnicity-specific disease associations. *Hum Mol Genet*. 2021;30(5):356–369.
22. Dik A, Widman G, Schulte-Mecklenbeck A, et al. Impact of T cells on neurodegeneration in anti-GAD65 limbic encephalitis. *Ann Clin Transl Neurol*. 2021;8(12):2289–2301.
23. Buniello A, MacArthur JAL, Cerezo M, et al. The NHGRI-EBI GWAS Catalog of published genome-wide association studies, targeted arrays and summary statistics 2019. *Nucleic Acids Res*. 2019;47(D1):D1005–D1012.
24. Weetman AP. An update on the pathogenesis of Hashimoto's thyroiditis. *J Endocrinol Invest*. 2021;44(5):883–890.
25. Jin Y, Birlea SA, Fain PR, et al. Variant of TYR and autoimmunity susceptibility loci in generalized vitiligo. *N Engl J Med*. 2010;362(18):1686–1697.
26. Jin Y, Birlea SA, Fain PR, et al. Genome-wide association analyses identify 13 new susceptibility loci for generalized vitiligo. *Nat Genet*. 2012;44(6):676–680.
27. Jin Y, Andersen G, Yorgov D, et al. Genome-wide association studies of autoimmune vitiligo identify 23 new risk loci and highlight key pathways and regulatory variants. *Nat Genet*. 2016;48(11):1418–1424.
28. Erlich H, Valdes AM, Noble J, et al. HLA DR-DQ haplotypes and genotypes and type 1 diabetes risk: analysis of the type 1 diabetes genetics consortium families. *Diabetes*. 2008;57(4):1084–1092.
29. Baschal EE, Aly TA, Babu SR, et al. Brief Report. *Diabetes*. 2007; 56-(September):2405–2409.
30. Flesch BK, Matheis N, Alt T, Weinstock C, Bux J, Kahaly GJ. HLA class II haplotypes differentiate between the adult autoimmune polyglandular syndrome types II and III. *J Clin Endocrinol Metab*. 2014;99(1):177–182.
31. Undlien DE, Friede T, Rammensee H-G, et al. HLA-Encoded Genetic Predisposition in IDDM: DR4 Subtypes May Be Associated With Different Degrees of Protection. *Diabetes*. 1997;46(1):143–149.
32. Angelini G, Morozzi G, Delfino L, et al. Analysis of HLA DP, DQ, and DR alleles in adult Italian rheumatoid arthritis patients. *Hum Immunol*. 1992;34(2):135–141.
33. Laroni A, Calabrese M, Perini P, et al. Multiple sclerosis and autoimmune diseases: Epidemiology and HLA-DR association in North-east Italy. *J Neurol*. 2006;253(5):636–639.
34. Ramos PS, Shedlock AM, Langefeld CD. Genetics of autoimmune diseases: Insights from population genetics. *J Hum Genet*. 2015; 60(11):657–664.
35. Jabrocka-Hybel A, Skalniak A, Piątkowski J, et al. How much of the predisposition to Hashimoto's thyroiditis can be explained based on previously reported associations? *J Endocrinol Invest*. 2018;41(12):1409–1416.
36. Kumasaka N, Fujisawa H, Hosono N, et al. PlatinumCNV: A Bayesian Gaussian mixture model for genotyping copy number polymorphisms using SNP array signal intensity data. *Genet Epidemiol*. 2011;35(8):831–844.